phys. stat. sol. (RRL) **1**, No. 6, 253–255 (2007) / **DOI** 10.1002/pssr.200701168

pss +++rapid research letters+++
www.pss-rapid.com

Local structure of interstitial Zn in β-Zn_4Sb_3

E. S. Toberer, K. A. Sasaki, C. R. I. Chisholm, S. M. Haile, W. A. Goddard III, and G. J. Snyder*

Materials Science, California Institute of Technology, Pasadena, CA 91126, USA

Received 31 July 2007, revised 19 September 2007, accepted 20 September 2007
Published online 25 September 2007

PACS 61.72.Ji, 66.30.Hs, 66.70.+f, 71.15.Mb

* Corresponding author: e-mail jsnyder@caltech.edu

The low thermal conductivity of the thermoelectric material β-Zn_4Sb_3 has been linked to disorder arising from multiple interstitial Zn sites. Here we investigate the energetics and local distortions associated with these interstitial sites *via* DFT calculations. Our results show the β-Zn_4Sb_3 structure is able to distort into many inequivalent geometries of similar energies, suggesting a topology rich with transport pathways through energetically accessible metastable states. The occurrence of such a shallow energy landscape may explain the recently discovered liquid-like diffusivity of Zn in β-Zn_4Sb_3 – comparable to that found in superionic conductors.

1 Introduction Zn_4Sb_3 is known to possess a high thermoelectric figure of merit in the 100–350 °C range, making it the most promising p-type material for waste heat recovery at these temperatures [1]. This excellent performance primarily arises from the extremely low lattice thermal conductivity in this material. A combination of reciprocal and real space diffraction analysis has been undertaken to identify the source of this low thermal conductivity and has identified both high levels of Zn disorder and Zn nanostructuring on the 5–10 nm length scales as sources of phonon scattering [2, 3]. In contrast, the Sb framework is very well ordered. As such, Zn_4Sb_3 represents one of the earliest "phonon-glass electron-crystal" structures discovered for thermoelectrics.

The low temperature α′- and α-phases and the high temperature β-phase of Zn_4Sb_3 have a framework composed of isolated and paired Sb atoms (here referred to as Sb1 and Sb2, respectively, following Ref. [2]), in which the Sb2 atoms are additionally each capped by three Zn1 atoms, Fig. 1a and b [4]. As such, the framework stoichiometry corresponds to $Zn_{12}Sb_{10}$.

In all three forms of Zn_4Sb_3, Zn additionally occupies interstitial sites thereby accommodating the final stoichiometry of $Zn_{13}Sb_{10}$ ($Zn_{3.9}Sb_3$). The phases are distinguished by the degree of interstitial ordering, with the α′- and α-phases exhibiting long range ordering of a five-atom interstitial cluster [4–6]. Grouping of interstitials at low temperatures (the α ↔ β transition occurs at ~250 K) is likely favoured due to the coupling of local framework distortions. Figure 1c shows how the interstitial sites may be characterized according to three basic structural motifs [2, 5]. The Zn2 interstitial is found at the head of the Sb2–Sb2 dimer as a fourth Zn atom, Zn3 is located in the gap between stacked dimers, and the Zn4 interstitial is equidistant from the dimer Sb2 atoms.

Given the significant structural distortions found in the α-structures which lower the overall symmetry from $R\bar{3}c$ in β ($a = 12.228$ Å, $c = 12.406$ Å) to $C\bar{1}$ in α ($a = 32.536$ Å, $b = 12.237$ Å, $c = 10.852$ Å, $\beta = 98.77°$) we anticipate Zn interstitials in the β-phase will induce the local $Zn_{12}Sb_{10}$ framework environment to similarly distort away from the refined $R\bar{3}c$ crystallographic positions. In this work, we utilize a triclinic (P1) cell to locate interstitial sites and reveal the changes in the local structure. These results lend insight into recent discoveries of extraordinarily fast diffusion of Zn ions and nanoscale ordering of interstitials in β-Zn_4Sb_3, as well as providing a framework for future calculations of transport and other properties.

2 Experimental Each of 19 trials started with 13 Zn atoms and 10 Sb atoms placed into the rhombohedral primitive cell of the β-structure. While Sb1 and Sb2 sites [2] were always used for antimony initial positions, the Zn

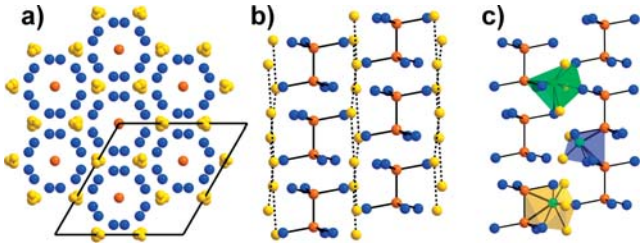

Figure 1 (online colour at: www.pss-rapid.com) Two views of the framework $Zn_{12}Sb_{10}$ structure are shown looking along the rhombohedral [100] (a) and [110] (b) directions. Sb2 atoms (orange) form dimers capped by Zn atoms (blue). Sb1 chains (yellow) are not bonding. (c) The three distinct interstitial sites in the high temperature β-phase as defined in Ref. [2]: Zn2 (green), Zn3 (blue), and Zn4 (yellow) polyhedra.

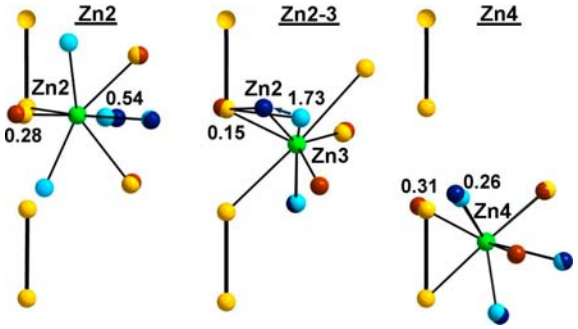

Figure 2 (online colour at: www.pss-rapid.com) Coordination around interstitial Zn atom (green) in three relaxed structures. Each cell began from the $Zn_{12}Sb_{10}$ structure (Sb: red, Zn: cyan) plus the interstitial, and converged into the relaxed structure (Sb: red, Zn: dark blue, interstitial: green). Insertion of a Zn atom at the Zn3 site induced the formation of an adjacent vacancy/Zn2 interstitial. The largest displacements are recorded in Å. Displacements <0.03 Å are shown as a single atom.

sites were varied. 16 of the trials contained all 12 Zn1 atoms plus one interstitial Zn atom. Adding the interstitial lowers the symmetry to P1 and brings the cell to the experimental stoichiometry of $Zn_{13}Sb_{10}$. Of these trials, three of the interstitial positions were from Snyder et al. [2] (Fig. 1c), three from Cargnoni et al. [7], one from analyzing void space in $Zn_{12}Sb_{10}$, and another nine taken from locations of residual density detected in the X-ray refinement [2]. The remaining three trials used multiple interstitial starting positions (removing an additional Zn1 to maintain the stoichiometry of $Zn_{13}Sb_{10}$), namely the BC and BCD structures of Cargnoni et al. [7], and Zn2 and Zn3 of Snyder et al. [2].

Atom positions were allowed to relax in SeqQuest [8], a fully self-consistent *ab initio* electronic structure code that uses Local Gaussian basis sets (contracted double zeta plus polarization quality) rather than plane waves in density functional theory (DFT) calculations to minimize the energy of atomic positions. All calculations used double-zeta plus polarization (DZP) basis sets [9]. Standard norm-conserving pseudopotentials were utilized, generated from Hamann's methods [10].

Initial calculations used the local density approximation (LDA). In all 19 distinct trials the cells were constrained in cell size and shape, but the struc-tures were allowed to relax to new atom positions. These final structures were then minimized again using Perdew–Burke–Ernzerhof pseudoatomic potentials [11] to obtain the final energies. Placing interstitial Zn atoms in crystallographically equivalent but physically distinct sites led to identical minimized energies (±1 meV/atom).

The 13 lowest energy structures are presented here, with energies represented in meV/atom above a stoichiometric ground state – treated here as the $Zn_{12}Sb_{10}$ structure plus the energy of a single atom of a Zn crystal.

3 Results and discussion Each of the initial cells converged to a distinct, energy-minimized structure. Of these structures, the lowest energy ones correlate closely to those obtained by electron density maps refined from X-ray diffraction [2]. The relaxed structures show final interstitial sites that can be generally identified with one of three possible positions, the distortions about which are shown in Fig. 2. These general low-energy interstitial positions are the same as those refined by Snyder et al. [2] but display induced distortions and vacancies in the local environment (distances shifted in the $Zn_{12}Sb_{10}$ framework indicated in Fig. 2). The insertion of a Zn atom into the Zn2 or Zn4 sites primarily distorts one Sb and one Zn neighbour. Insertion of a interstitial onto the Zn3 site causes an adjacent Zn1 atom to shift onto a Zn2 interstitial position, creating a vacancy and a Zn2–3 interstitial pair. All relaxed structures containing a Zn3 interstitial were paired with an additional interstitial and a vacancy. These results are consistent with the observed 90% occupancy of the Zn1 site. The relaxation of local atoms results in minimum Zn–Zn distances of approximately 2.4 Å, compared to the 2.2 Å in Cargnoni et al. [7].

Figure 3a shows the distribution of energies observed for various final structures. In all cases, the structure is able to lower its energy by relaxing the atoms coordinating the interstitial. The wide variety of geometrically unique local distortions gives rise to the observed range of energies in Fig. 3a. The energies are shown relative to the relaxed Zn2 interstitial which was the lowest energy β-phase structure found. The three primary interstitial structures (Zn2, Zn2–3, Zn4 as shown in Fig. 2) all have comparable energetics, in agreement with the occupancy of all three sites in the σ- and β-phases. Spontaneous formation of the α-phase cannot be observed in our structure as long-range correlations in excess of our unit cell (>10 Å) are inaccesible.

DFT calculations using the α-structure have found this low temperature phase should be unstable towards disproportionation into 10ZnSb + 3Zn [4]. Prior calculations have shown that the formation of β-cell structures containing interstitials is likewise unfavourable [7]. Those results have led to the conclusion that the β-phase must be highly entropy-stabilized and that the ordered α-structures are

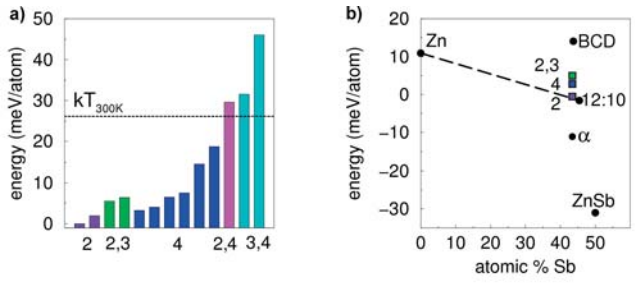

Figure 3 (online colour at: www.pss-rapid.com) (a) Energies of the relaxed $Zn_{13}Sb_{10}$ structures, grouped by nomenclature of [2] (see Fig. 1). The "2,3" and "3,4" structures contain two interstitials bonded to the same dimer while the "2,4" structure spans two adjacent dimers. The dotted line represents kT at room temperature, relative to the lowest energy β-phase structure. (b) Energetics of the Zn–Sb system, relative to the energy of Zn + $Zn_{12}Sb_{10}$. From (a), only the lowest energy from the "2", "2,3", "4" groupings is shown. Energies for ZnSb, the α-phase, and the BCD β-phase from the Refs. [4, 7].

metastable [4]. In this work and in prior work by Cargnoni et al., the various relaxed structures are all energetically unfavourable compared to $Zn_{12}Sb_{10}$ + Zn, again suggesting entropic stabilization of $Zn_{13}Sb_{10}$. The relative energies are shown in Fig. 3b, with our three lowest energy Zn2, 2/3, and 4 structures overlaid on the results of Cargnoni et al. and Mikhaylushkin et al. [4, 7].

The presence of so many metastable structures below $kT_{300\,K}$ is consistent with the high Zn diffusion rates found in β-Zn_4Sb_3, as measured by tracer diffusion experiments [12]. At 270 °C, the diffusion coefficient of Zn is found to be 1.2×10^{-6} cm^2/s. This remarkably high value is comparable to that of the fast-ion conductor AgI in the 'superionic' phase ($D_{Ag} \approx 2.1 \times 10^{-5}$ cm^2/s at 250 °C [13]). Such high diffusion rates suggest the Zn motion is enabled by the presence of multiple interstitial sites with equivalent energies and low potential barriers between sites (activation energy Zn: 11 kJ/mol; Ag in AgI: 9 kJ/mol [14]). The mobile species in such superionic conductors are often described as 'liquid-like' and the order–disorder transition described as 'sublattice melting' [15]. While it is unclear whether such terms apply to β-Zn_4Sb_3, the results here suggest substantial analogies.

Real-space X-ray and neutron analysis using the pair-distribution function (PDF) method has led to further insight into both the low and high temperature Zn_4Sb_3 phases [3]. These methods have confirmed that the phases are extremely structurally similar, including the nature of their interstitial geometry. The most relevant result from the PDF measurements is an envelope function for the β-phase which is indicative of a lower symmetry, locally ordered α-like structure which does not have long range coherency (<10 nm). Unfortunately, because of the many similar bond distances that occur in the structure, the exact nature of the interstitial coordination is not revealed. Spatial and temporal fluctuations in the domain structure can then give rise to the observed high Zn diffusivity. Analogous behaviour has been observed in 'cubic' ferroerroelectrics which are described as averages of lower symmetry nanodomains [16]. Fluctuating nanodomains would further be expected to readily scatter longer wavelength acoustic phonons which are largely responsible for heat transport.

4 Conclusion By relaxing a number of distinct initial interstitial β-Zn_4Sb_3 structures, we have identified several energetically accessible, geometrically unique metastable interstitial/vacancy structures. The occurrence of such structures and the interstitial disorder may explain both the remarkably high 'liquid-like' Zn diffusivity and the presence of α-like nanodomains in the β-structure. Perhaps most importantly, these features may be responsible for the exceptionally low thermal conductivity of β-Zn_4Sb_3.

Acknowledgements We are grateful for the assistance of Timo Jacob and Yuki Matsuda in this work. We thank JPL-NASA, the National Science Foundation and the Beckman Institute at Caltech for funding.

References

[1] T. Caillat, J. P. Fleurial, and A. Borshchevsky, J. Phys. Chem. Solids **58**, 1119–1125 (1997).
[2] G. J. Snyder, M. Christensen, E. Nishibori, T. Caillat, and B. B. Iversen, Nature Mater. **3**, 458–463 (2004).
[3] H. J. Kim, E. S. Božin, S. M. Haile, G. J. Snyder, and S. J. L. Billinge, Phys. Rev. B **75**, 134103 (2007).
[4] A. S. Mikhaylushkin, J. Nylén, and U. Häussermann, Chem. Eur. J. **11**, 4912–4920 (2005).
[5] J. Nylén, S. Lidin, M. Andersson, B. B. Iversen, H. Liu, N. Newman, and U. Häussermann, Chem. Mater. **19**, 834–838 (2007).
[6] J. Nylén, M. Andersson, S. Lidin, and U. Häussermann, J. Amer. Chem. Soc. **126**, 16306–16307 (2004).
[7] F. Cargnoni, E. Nishibori, P. Rabiller, L. Bertini, G. J. Snyder, M. Christensen, C. Gatti, and B. B. Iversen, Chem. Eur. J. **10**, 3861–3870 (2004).
[8] P. A. Schultz, unpublished results; a description of the method is in: P. J. Feibelman, Phys. Rev. B **35**, 2626–2646 (1987).
[9] A. E. Mattsson, P. A. Schultz, M. P. Desjarlais, T. R. Mattsson, and K. Leung, Model. Simul. Mater. Sci. Eng. **13**, R1–R31 (2005).
[10] D. R. Hamann, Phys. Rev. B **40**, 2980 (1989).
[11] J. P. Perdew, K. Burke, and M. Ernzerhof, Phys. Rev. Lett. **77**, 3865–3868 (1996).
[12] E. Chalfin, H. Lu, and R. Dieckmann, Solid State Ion. **178**, 447–456 (2007).
[13] G. Eckold, K. Funke, J. Kalus, and R. E. Lechner, J. Phys. Chem. Solids **37**, 1097–1103 (1976).
[14] V. I. Polyakov, Russ. J. Phys. Chem. **72**, 1812 (1998).
[15] M. O'Keeffe and B. G. Hyde, Philos. Mag. **33**, 219–224 (1976).
[16] H. Krakauer, R. C. Yu, C. Z. Wang, K. M. Rabe, and U. V. Waghmare, J. Phys.: Condens. Matter **11**, 3779–3787 (1999).